



HAL
open science

Observational constraints on cosmological future singularities

Jose Beltrán Jiménez, Ruth Lazkoz, Diego Sáez-Gómez, Vincenzo Salzano

► **To cite this version:**

Jose Beltrán Jiménez, Ruth Lazkoz, Diego Sáez-Gómez, Vincenzo Salzano. Observational constraints on cosmological future singularities. *European Physical Journal C: Particles and Fields*, 2016, 76 (11), pp.631. 10.1140/epjc/s10052-016-4470-5 . hal-01282516

HAL Id: hal-01282516

<https://hal.science/hal-01282516>

Submitted on 3 Mar 2016

HAL is a multi-disciplinary open access archive for the deposit and dissemination of scientific research documents, whether they are published or not. The documents may come from teaching and research institutions in France or abroad, or from public or private research centers.

L'archive ouverte pluridisciplinaire **HAL**, est destinée au dépôt et à la diffusion de documents scientifiques de niveau recherche, publiés ou non, émanant des établissements d'enseignement et de recherche français ou étrangers, des laboratoires publics ou privés.

Observational support for approaching cosmic doomsday

Jose Beltrán Jiménez,¹ Ruth Lazkoz,² Diego Sáez-Gómez,³ and Vincenzo Salzano⁴

¹*CPT, Aix Marseille Université, UMR 7332, 13288 Marseille, France*

²*Fisika Teorikoaren eta Zientziaren Historia Saila, Zientzia eta Teknologia Fakultatea, Euskal Herriko Unibertsitatea, 644 Posta Kutxatila, 48080 Bilbao, Spain*

³*Instituto de Astrofísica e Ciências do Espaço, Departamento de Física, Faculdade de Ciências da Universidade de Lisboa,*

Edifício C8, Campo Grande, P-1749-016 Lisbon, Portugal

⁴*Institute of Physics, University of Szczecin, Wielkopolska 15, 70-451 Szczecin, Poland*

(Dated: February 22, 2016)

In this work we consider a family of cosmological models featuring future singularities. This type of cosmological evolution is typical of dark energy models with an equation of state violating some of the standard energy conditions (e.g. the null energy condition). Such kind of behavior, widely studied in the literature, may arise in cosmologies with phantom fields, theories of modified gravity or models with interacting dark matter/dark energy. We briefly review the physical consequences of these cosmological evolutions regarding geodesic completeness and the divergence of tidal forces in order to emphasize under which circumstances the singularities in some cosmological quantities correspond to actual singular spacetimes. We then introduce several phenomenological parameterizations of the Hubble expansion rate to model different singularities existing in the literature and use SN Ia, BAO and $H(z)$ data to constrain how far in the future the singularity needs to be (under some reasonable assumptions on the behaviour of the Hubble factor). We show that quite generally, the lower bound for the singularity time can not be smaller than about 1.2 times the age of the universe, what roughly speaking means ~ 2.8 Gyrs from the present time.

I. INTRODUCTION

The standard model of cosmology together with the inflationary paradigm provide an accurate description of the universe, although it requires the presence of three unknown ingredients, namely: Dark matter, dark energy and the inflaton field. The last two share the property of being introduced in order to support phases of accelerating expansion. Moreover, while the inflaton accounts for the first instants of life of our universe, dark energy should determine its final fate as the component that will eventually dominate. If dark energy turns out to be simply a cosmological constant, then we are doomed to an asymptotically de Sitter universe in the future. The situation is much more subtle when dynamical dark energy or modified gravity is brought in as possible explanations for the late time accelerated expansion (for a review about dark energy models, see [1]). In some cases, dark energy is ascribed to a so-called phantom fluid, i.e., a fluid satisfying $\rho + p < 0$ and, thus, violating the Null Energy Condition (NEC) [2]. For a set of minimally coupled scalar fields, this condition implies the presence of, at least, a laplacian instability in the inhomogeneous perturbations, although this can be resolved by allowing non-minimal couplings (see for instance [3]). Moreover, such kind of behavior can be also a consequence of a modification of General Relativity instead of a fluid with a non-standard equation of state [4]. In any case, the phantom behavior may affect the background evolution giving rise to a future singularity occurring at a finite time where the scale factor diverges. Nevertheless, note that some models with violations of the null energy condition do not drive the universe to a singularity but to regular scenar-

ios that may affect the local structures, known as *little Rip*, *Pseudo-Rip* and *Little Sibling* [5–7].

The described singular behaviour is actually shared by many dynamical dark energy models and modified gravity scenarios, where divergences in different cosmological parameters at a finite time can appear. The nature of the future singularities may differ among the different scenarios and they can be classified according to the cosmological parameters that diverge. An alternative way of classifying the future singularities is by means of the derivative of the scale factor that diverges. This classification is very useful because it helps understanding the severity of the different types of singularities (for a classification of cosmological singularities, see Ref. [8, 9]). At this respect, it is worth reminding that a singular spacetime is characterized by the incompleteness of the geodesics [10]. Since the geodesic equations are linear in the connection, it will contain, at most, first derivatives of the metric. Thus, the geodesics will be regular as long as the metric is continuous at the singularity. For a cosmological model, this will mean that the scale factor should remain finite at the singularity, even if divergences in the Hubble expansion rate or its derivatives are present. This type of behaviour has been recently used in [11] in order to replace the Big Bang singularity with a milder one that can be trespassed by the geodesics.

Another useful equation in order to characterize the strength of a singularity is the geodesics deviation equation. That equation essentially determines the tidal forces suffered by two infinitesimally close geodesics and it depends on the curvature of the spacetime. This means that tidal forces are sensitive to singularities which do not necessarily affect the completeness of the geodesics. Again

in a cosmological context, if the scale factor remains regular, but the Hubble rate diverges, it is possible to have a regular geodesic congruence with divergent tidal forces. Some criteria based on the behaviour of the Riemann tensor as we approach the singularity exist in the literature to decide whether the singularity is strong or weak, being the Tipler [12] and Krolak [13] conditions two widely used ones.

Regardless the physical consequences of having a future singularity at a finite time, a natural question to ask is how close a given type of singularity is to us [14]. This is the analogous of asking about the age of the universe, determined by our distance to the original Big Bang singularity. Nevertheless, in the same way as we do not expect the Big Bang singularity to exist actually, but rather being regularized by some quantum effects, high curvature corrections to Einstein's gravity or even by varying physical constants [15], we do not expect the future singularities to be physical, at least the strongest types where physical quantities diverge [16]. However, it will be useful to have some estimation on how close to us a given singularity can be and, therefore, have an idea of how far in the future we could extrapolate a model with a certain type of future singularity. It is important to notice that an effective equation of state for dark energy $w < -1$ is within the confidence regions of observational data [17] so the possibility of having a future singularity is plausible. Moreover, such models have also received attention because of some theoretical implications, since possible quantum effects close to the singularity become important. We know that General Relativity is to be regarded as an effective field theory whose strong coupling scale is, in the most optimistic scenario, at the Planck scale. Thus, knowing at which time the singularity is essentially reached will give us also an idea of until when we can keep using General Relativity as an effective field theory.

The purpose of the present work is precisely to draw such an estimation in a fairly model independent framework. An important difficulty arising here with respect to the Big Bang case is that, while in that case we have control on the different phases that the universe has gone through from the initial singularity until today, for the future singularity we cannot know what the future phases will be. Thus, we need to make some assumptions to eventually determine how close the singularity can be. In order to achieve this, we will use some classes of phenomenological parameterizations for the Hubble expansion rate as proxies for a universe with a transition from a matter dominated era to a dark energy phase leading to a future singularity. We will then confront them to SN Ia, BAO and $H(z)$ data to obtain the time of the singularity. Obviously, there could be transient phases that could delay the singularity, but this will not concern us since we are actually interested in obtaining a general lower bound for a future singularity.

The paper is organized as follows: section II is devoted

to a brief review about future cosmological singularities. In section III, the parametrizations of the Hubble rate which are analyzed in the paper are introduced. Then, the observational data used to fit the models is described in section IV. Finally, section V is devoted to the results discussions.

II. FUTURE COSMOLOGICAL SINGULARITIES

Assuming an homogeneous and isotropic universe at large scales, in compliance with the cosmological principle, the metric is given by the Friedmann-Lemaître-Robertson-Walker (FLRW) line element which is expressed as follows

$$ds^2 = -dt^2 + a(t)^2 (dx^2 + dy^2 + dz^2) , \quad (1)$$

where we have assumed spatial flatness. Within General Relativity and assuming a perfect fluid as matter source, the gravitational equations can be written as

$$H^2 = \frac{8\pi G}{3}\rho , \quad \dot{H} = -4\pi G(\rho + p) . \quad (2)$$

Here ρ and p are the energy and pressure densities respectively of the perfect fluid, while $H = \frac{\dot{a}}{a}$ is the Hubble parameter. These equations are enough to describe the background cosmological evolution once the matter content of the universe is specified. In addition to these equations, the Bianchi identities allow to obtain the continuity equation $\dot{\rho} + 3H(\rho + p) = 0$, which is nothing but the field equations of the matter sector. For an arbitrary and constant equation of state (EoS) parameter $w \equiv p/\rho \neq -1$, the continuity equations can be easily integrated to give $\rho \propto a^{-3(1+w)}$ so that the above equations yield the familiar solutions:

$$H = \frac{2}{3(1+w)(t-t_s)} \Rightarrow a(t) \propto (t-t_s)^{\frac{2}{3(1+w)}} \quad (3)$$

with t_s some integration constant. For $w > -1$ this equation contains a singularity at $t = t_s$, where $a \rightarrow 0$ and the energy density $\rho \propto a^{-3(1+w)}$ diverges, which corresponds to the Big Bang or Big Crunch singularities. On the other hand, when $w < -1$, the above solution would lead to a contracting universe unless $t < t_s$ which corresponds to an expanding universe that ends in a future singularity at the Rip time t_s where the energy density diverges but also the scale factor. This is the so-called Big Rip singularity, which has drawn much attention over the last years since dark energy models with an EoS parameter $w < -1$ (usually called phantom) are allowed by the observations constraining the homogeneous background evolution, as we have commented upon before. However, although this is possibly the simplest type of future singularity, it is not the only possible one and, in fact, a relatively large amount of different future singularities have been found in more contrived cosmological scenarios based on non-standard fields, more general fluids or

modified gravity. The different types of finite late-time singularities can be classified according to the divergent cosmological quantity at the singularity as follows (see Refs. [8, 9],

- Type I (“Big Rip singularity”): For $t \rightarrow t_s$, $a \rightarrow \infty$ and $\rho \rightarrow \infty$, $|p| \rightarrow \infty$. Time-like geodesics are incomplete [14, 18].
- Type II (“Typical Sudden singularity”): For $t \rightarrow t_s$, $a \rightarrow a_s$ and $\rho \rightarrow \rho_s$, $|p| \rightarrow \infty$. Geodesics are not incomplete. This is classified as a weak singularity (see Ref. [19]).
- Type III (“Big freeze”): For $t \rightarrow t_s$, $a \rightarrow a_s$ and $\rho \rightarrow \infty$, $|p| \rightarrow \infty$. No geodesics incompleteness. They can be weak or strong (see Ref. [20]).
- Type IV (“Generalized Sudden singularity”): For $t \rightarrow t_s$, $a \rightarrow a_s$ and $\rho \rightarrow \rho_s$, $p \rightarrow p_s$ but higher derivatives of Hubble parameter diverge. They are weak singularities [21].
- Type V (“ w -singularities”): For $t \rightarrow t_s$, $a \rightarrow \infty$ and $\rho \rightarrow 0$, $|p| \rightarrow 0$ and $w = p/\rho \rightarrow \infty$. These singularities are weak (see Ref. [22]).

In addition, there are other scenarios where no quantity diverges at a finite time but at infinity, namely the “Little Rip” [5], “Pseudo-Rip” [6] and “Little Sibling” [7]. The above classification is useful since it groups together different models exhibiting a background evolution where some cosmological quantity meets a divergence in the future. The fact that some given quantities might have a divergence is usually regarded as a non-desirable feature to have in a regular spacetime. However, a regular spacetime is only defined in terms of its geodesic completeness. Thus, a spacetime with a curvature divergence can be regular as long as the geodesics can *smoothly* go through the divergence. Hence, cosmological models with some of the divergences in the above classification do not need to correspond to singular spacetimes and, consequently, singular future universes. In order to study whether the different singularities correspond to a geodesically incomplete spacetime we will consider the geodesic equations given by

$$\frac{dx^\mu}{d\lambda^2} + \Gamma_{\alpha\beta}^\mu \frac{dx^\alpha}{d\lambda} \frac{dx^\beta}{d\lambda} = 0 \quad (4)$$

where λ is some affine parameter (proper time for instance for non-null geodesics) and $\Gamma_{\alpha\beta}^\mu$ are the corresponding Christoffel symbols. This equation already shows that it is the connection which determines the smoothness of the geodesics. In general, the solutions of the differential equations will be better behaved than the coefficients of the equations, so it is plausible to have a divergence in the connection with the geodesics remaining well-defined. It is also important to notice that the curvature contains derivatives of the connection and, therefore, there can be situations with curvature divergences, but

where the connection (and consequently the geodesics) are perfectly regular. We will illustrate this below for some specific cases. The relevant case for the cosmological evolution is a spacetime described by the FLRW metric. In that case, the geodesic equations read¹

$$\frac{d^2 t}{d\lambda^2} + H a^2 \delta_{ij} \frac{dx^i}{d\lambda} \frac{dx^j}{d\lambda} = 0, \quad (5)$$

$$\frac{d^2 x^i}{d\lambda^2} + 2H \frac{dx^i}{d\lambda} \frac{dt}{d\lambda} = 0. \quad (6)$$

These equations can be easily integrated. We start by rewriting the Hubble parameter in terms of the affine parameter as

$$H = \frac{\dot{a}}{a} = \frac{1}{a} \frac{da/d\lambda}{dt/d\lambda}. \quad (7)$$

Then, we can rewrite Eq. (6) as

$$\frac{d}{d\lambda} \left(a^2 \frac{dx^i}{d\lambda} \right) = 0 \quad (8)$$

which can be immediately integrated to obtain

$$\frac{dx^i}{d\lambda} = \frac{u_0^i}{a^2} \quad (9)$$

with u_0^i some integration constants. We can then use this solution into Eq. (5) to obtain

$$\left(\frac{dt}{d\lambda} \right)^2 = \frac{|\vec{u}_0|^2}{a^2} + C_0 \quad (10)$$

where C_0 is another integration constant. We thus see that the geodesics will be regular (with a well-defined tangent vector) as long as the scale factor remains regular. If the scale factor does not diverge and is non-vanishing (so the metric is regular) the 4-velocities of the geodesics remain regular and the spacetime will be said to be non-singular. If the scale factor diverges at some point, then the geodesics stop there and cannot go through it. As we have discussed above, it is important to notice that the geodesics are insensitive to divergences in the expansion rate H or its derivatives if they do not correspond to a singular behavior of the scale factor. This will be the case of the types II, III and IV singularities in the above classification where the scale factor remains finite while all the divergences only appear in its derivatives.

So far we have discussed the singularities from the point of view of geodesic completeness. Another class of criteria that is useful to study the presence of a singular physical behaviour is the geodesic deviation equation, which allows to infer the potential existence of divergences in tidal forces. The corresponding equations

¹ Here we will focus on spatially-flat universes. For the general case see [23]

depend on the Riemann tensor, which explicitly contains the Hubble expansion rate and its first time-derivative so that it is, in principle, sensitive to divergences that do not affect the geodesics themselves. Two common criteria to classify these divergences are the so-called strong curvature divergences in the Tipler and Krolak sense, which are respectively characterized by the following integrals:

$$T(u) \equiv \int_0^\lambda d\lambda' \int_0^{\lambda'} d\lambda'' R_{ij} u^i u^j, \quad (11)$$

$$K(u) \equiv \int_0^\lambda d\lambda''' R_{ij} u^i u^j. \quad (12)$$

with u^i the 4-velocity of the geodesic approaching the singularity. Here again we see that divergences in the curvature do not necessarily lead to a physical singularity because integrals of a given function are generally better behaved than the function itself. Thus, even if the spacetime contains a curvature divergence, it can remain *regular* according to the above criteria. The physical reason roots in the fact that the geodesic deviation equation measures the infinitesimal deviation, i.e., the tidal force between infinitesimally closed geodesics. However, extended physical objects have a finite physical volume and the above criteria precisely give the conditions for a finite volume to remain finite when going through the singularity. On the other hand, if the tidal forces are strong enough such that the volume shrinks to zero, the singularity is said to be strong.

III. THE MODELS

In this section we will describe the parameterizations that we will use for the subsequent confrontation to observational data. We emphasize that we intend to establish a general lower bound for the time of the future singularity t_s in a fairly model independent manner. Since we are dealing with future singularities occurring at a finite proper time, it is reasonable to perform our parameterizations in terms of proper time. Moreover, as we have discussed, the severity of the different types of singularities is essentially determined by whether the scale factor or any of its time-derivatives presents a divergence. Therefore, the natural cosmological quantity to parameterize is the scale factor. However, for convenience when confronting to SN Ia and BAO, it will be more appropriate to parameterize the Hubble expansion rate directly. By doing this, we also avoid the ambiguity in the normalization of the scale factor.

As commented in the introduction, the main difficulty with respect to constraining the time of the Big Bang is that, while we have an accurate knowledge about the past history of the universe so we can robustly compute such a time, the future evolution of the universe is completely unknown. Because of that we need to make some relatively strong assumptions on our parameterizations. First of all, we want to have an approximate matter

dominate phase at early times; we will use low-redshift ($z < 2$) cosmological data so that by early time we actually mean well inside the matter domination epoch, but much later than equality and decoupling times, i.e., redshifts $10 \leq z \leq 1000$. In order to comply with this requirements we propose to use the following form for the Hubble expansion rate:

$$H(t) = \frac{2}{3t} + F(t, t_s), \quad (13)$$

where t_s is the time when one of the above singularities occur and the function $F(t, t_s)$ is assumed to be negligible for $t \ll t_0$ with t_0 the present time, such that $H(t \ll t_0) \simeq \frac{2}{3t}$ as it corresponds for a matter dominated universe. In terms of the scale factor, this translates into a parameterization of the form

$$a(t) \propto g(t, t_s) t^{2/3} \quad \text{with} \quad F(t, t_s) = \frac{\dot{g}}{g}. \quad (14)$$

This matter dominated phase will then be matched to an evolution with a future time singularity, i.e., $F(t, t_s)$ is a function that either itself or some of its time-derivatives diverges at $t = t_s$. Since we are looking for a future divergence where a given derivative of the scale factor diverges while the lower derivatives remain finite, a reasonable Ansatz for $F(t, t_s)$ is some half-integer power. The specific parameterizations that we have chosen are summarized in Table. I together with their main properties, where the type of singularity is provided. All the models contain two parameters characterizing the time of the singularity t_s and an additional parameter n that regulates the time of the transition from matter domination. Notice that all the parameterizations share the property of containing a late-time de Sitter evolution when the time of the singularity is sent to the asymptotic future² $t_s \rightarrow \infty$. However, it is important to notice that the existence of a matter phase at early times matching a de Sitter universe in the asymptotic future does not necessarily mean that the evolution mimics that of a Λ CDM model, because the transition era between the two phases may be completely different. In fact, it is not difficult to see that none of our parameterizations contains Λ CDM within its parameter space.

A noteworthy feature of our parameterizations is that they are introduced at the level of the Hubble expansion parameter directly, unlike some previous studies that parameterize some dynamical quantities associated to the matter sector, be it the equation of state or the energy density directly [24]. In those cases, one needs to resort to some underlying gravitational theory (usually assumed to be General Relativity). Our results however will be independent of any assumptions about the gravitational

² For the model *C* we need to simultaneously send n to infinity so that the product $n \log(1 - t/t_s)$ remains finite.

theory, only requiring that it is metric so particles follow geodesics in a FLRW universe. Therefore, our results will apply to a very large class of models as long as the cosmological evolution is well captured by one of our parameterizations. Let us stress however that we do not expect our parameterizations to be exact solutions of any theoretical model, but simply approximate analytical expressions describing the true solutions.

As we have said, we do not need to rely on any gravitational theory for our parameterizations. However, in order to make contact with previous literature and give a physical intuition of what kind of theoretical models might be described by our parameterizations, we will now consider some explicit cases.

If we assume General Relativity for the gravitational interaction, then Friedmann equation directly relates the Hubble expansion rate to the total energy density of the universe as

$$H^2 = \frac{8\pi G}{3}\rho. \quad (15)$$

where ρ collectively represents all the possible components in the universe. From the second gravitational equation we can relate the Hubble expansion rate to the pressure as

$$2\dot{H} + 3H^2 = -8\pi Gp \quad (16)$$

where, again, p comprises all the species with pressure in the universe. These two equations allow to obtain an effective equation of state parameter w_{eff} in terms of the Hubble expansion rate and its derivative as

$$w_{\text{eff}} \equiv \frac{p}{\rho} = -1 - \frac{2}{3}\frac{\dot{H}}{H^2}. \quad (17)$$

Thus, we can interpret our parameterizations in terms of an effective equation of state parameter for the content of the universe, assuming a perfect fluid form and a barotropic equation of state. Since at early times our parameterizations give $H \simeq 2/(3t)$, we recover a matter dominated universe with $w_{\text{eff}} \simeq 0$ as it should.

IV. DATA

The analysis has been performed using three different standard cosmological tools. They are at low redshift ($z \lesssim 2$), because we are not interested in changing early time evolution and we assume that a possible signature for “future” evolution toward a singularity, if any, is detectable now or, at least, in the recent past only.

Just for sake of clarity and computational motivations, all the models we propose are written in terms of the dimensionless variable $x = t/t_0$, where t_0 is the age of the Universe. This means that all quantities will be measured in units of t_0 so, for instance, we will have

$$H(t) = \frac{H(x)}{t_0}. \quad (18)$$

Therefore, in this case t_0 plays, in terms of fitting parameters, the role usually ascribed to the Hubble constant H_0 in the standard approach.

Since our parameterizations are explicitly expressed in terms of time, it will be more convenient to use all the standard integrals involved in the calculation of cosmological distances directly expressed as integrations over time, instead of transforming them into integrations over redshift, being the two of them related as

$$\int_0^z \frac{d\tilde{z}}{H(\tilde{z})} \rightarrow \int_1^x \frac{d\tilde{x}}{a(\tilde{x})}. \quad (19)$$

The integrations over redshift are more convenient in the usual case because the observational data are given in terms of redshift. Thus, we will need to find the values of x that correspond to the given redshifts, i.e., we need to find the functions $z = z(x)$ or, equivalently $a = a(x)$. This can be easily obtained from the corresponding expression for $H(x)$ by solving the differential equation

$$H(x) = \frac{a'(x)}{a(x)}, \quad (20)$$

where the prime stands for derivative with respect to x . This equation will be solved with the boundary condition $a(x=1) = 1$, i.e., we normalize the scale factor to be 1 today. Thus we operationally define the time t_0 in our models by such condition. Notice that for all our parameterizations this can be done analytically. Therefore, we can obtain the values of x_i corresponding to the measured values z_i by numerically solving the equation $z_i = 1/a(x_i) - 1$.

A. Hubble data from early-type galaxies

We use the compilation of Hubble parameter measurements estimated with the differential evolution of passively evolving early-type galaxies as cosmic chronometers, in the redshift range $0 < z < 1.97$ and recently updated in [25]. The corresponding χ_H^2 estimator is defined as

$$\chi_H^2 = \sum_{i=1}^{24} \frac{(H(x_i, \boldsymbol{\theta}) - H_{\text{obs}}(x_i))^2}{\sigma_H^2(x_i)}, \quad (21)$$

with $\sigma_H(z_i)$ the observational errors on the measured $H_{\text{obs}}(z_i)$ values, and $\boldsymbol{\theta}$ is the vector of cosmological parameters, i.e., (t_0, n, t_s) in our case. Moreover, we will add a gaussian prior, derived from the Hubble constant value given in [26], $H_0 = 69.6 \pm 0.7$. Notice that now H_0 is a derived quantity depending on the actual fitting parameters so

$$H_0 = H_0(\boldsymbol{\theta}) = \frac{H(x=1, \boldsymbol{\theta})}{t_0}, \quad (22)$$

where the numerator $H(x=1, \boldsymbol{\theta})$ now depends on the parameters n and x_s .

| our | N.O.T. | $H(x)$ | $a(x)$ | a | H | \dot{H} | \ddot{H} | ρ | p | w_{eff} |
|-----|--------|-------------------------------------------------------------------|-------------------------------------------------------------------------------------|----------|-----------|-----------------|------------|----------|-----------|------------------|
| A | I | $\frac{2}{3x} + \frac{2n}{3(1-x/x_s)}$ | $a_0 x^{\frac{2}{3}} (x_s - x)^{-\frac{2}{3} \cdot n x_s}$ | ∞ | ∞ | ∞ | ∞ | ∞ | $-\infty$ | $w_s < 0$ |
| B | III | $\frac{2}{3x} + \frac{2n}{3\sqrt{1-x/x_s}}$ | $a_0 x^{\frac{2}{3}} \exp[-\frac{4}{3}n\sqrt{x/x_s}(x_s-x)]$ | a_s | ∞ | ∞ | ∞ | ∞ | $-\infty$ | $-\infty$ |
| C | III | $\frac{2}{3x} - \frac{2n}{3} \log\left(1 - \frac{x}{x_s}\right)$ | $a_0 x^{\frac{2}{3}} \exp[-\frac{2}{3}n(x-x_s)(-1 + \log[1-x/x_s])]$ | a_s | ∞ | ∞ | ∞ | ∞ | $-\infty$ | $-\infty$ |
| D | II | $\frac{2}{3x} + \frac{2n}{3}\sqrt{1-x/x_s}$ | $a_0 (x/x_s)^{\frac{2}{3}} \exp[-\frac{4}{9} \cdot n x_s (1-x/x_s)^{\frac{3}{2}}]$ | a_s | $H_s > 0$ | $-\infty$ | $-\infty$ | ρ_s | ∞ | ∞ |
| E | IV | $\frac{2}{3x} + \frac{2n}{3}\left(1 - \frac{x}{x_s}\right)^{3/2}$ | $a_0 (x/x_s)^{\frac{2}{3}} \exp[-\frac{4}{15} \cdot n x_s (1-x/x_s)^{\frac{5}{2}}]$ | a_s | $H_s > 0$ | $\dot{H}_s < 0$ | ∞ | ρ_s | 0 | 0 |

Table I. In this table we summarize the 5 parameterizations that we propose to describe the different types of future singularities that we consider throughout this work. In the first column we give the label we will use for each case, while the second column indicates the type of singularity according to the classification in [8]. In the columns 3 and 4 we give the analytical expressions for $H(t)$ and $a(t)$ (where, as explained in the main text, the normalization a_0 must be chosen so that $a(x=1)=1$). In the last columns we give the behaviour of a , H and some of its derivatives at the singularity. We also give the values of ρ , p and w_{eff} for the theoretical interpretation discussed in Section III. It is important to keep in mind that those values depend on the underlying theoretical model and we only give them here for illustrative purposes.

B. Type Ia Supernovae

We use the SN Ia data from the Union2.1 compilation [27]. The χ_{SN}^2 in this case is generally defined as

$$\chi_{SN}^2 = \Delta \mathcal{F}^{SN} \cdot \mathbf{C}^{-1} \cdot \Delta \mathcal{F}^{SN}, \quad (23)$$

with $\Delta \mathcal{F}^{SN} = \mu_{theo} - \mu_{obs}$ the difference between the observed and theoretical value of the distance modulus μ , the observable quantity for Union2.1 SN Ia, defined as:

$$\mu = 5 \log_{10}[d_L(z, \boldsymbol{\theta})] + \mu_0; \quad (24)$$

with $d_L(z)$ the dimensionless luminosity distance given by

$$d_L(z, \boldsymbol{\theta}) = (1+z) \int_0^z \frac{d\tilde{z}}{E(\tilde{z}, \boldsymbol{\theta})}, \quad (25)$$

where $E(z) = H(z)/H_0$ is the dimensionless Hubble function; μ_0 a nuisance parameter combining the Hubble constant H_0 (or t_0 in our case) and the absolute magnitude of a fiducial SN Ia. As usual, we marginalize the χ_{SN}^2 over μ_0 . Finally, \mathbf{C} is the covariance matrix. In terms of integration over time, the dimensionless luminosity distance can be expressed as:

$$d_L(x, \boldsymbol{\theta}) = \frac{1}{a(x, \boldsymbol{\theta})} \int_1^x \frac{d\tilde{x}}{a(\tilde{x}, \boldsymbol{\theta})}. \quad (26)$$

C. Baryon Acoustic Oscillations

We have also made use of baryon acoustic oscillations (BAO), in particular, the data collected in [28]. In this case the χ_{BAO}^2 is defined as

$$\chi_{BAO}^2 = \Delta \mathcal{F}^{BAO} \cdot \mathbf{C}^{-1} \cdot \Delta \mathcal{F}^{BAO}, \quad (27)$$

where, as before, $\Delta \mathcal{F}^{BAO} = F_{theo} - F_{obs}$ is the difference between the observed and theoretical value of the Alcock-Paczynski distortion parameter measured in a BAO survey, and defined as:

$$F(z) = (1+z) D_A(z) \frac{H(z)}{c}, \quad (28)$$

with c the speed of light, $H(z)$ the Hubble function, and D_A the angular diameter given by:

$$D_A(z, \boldsymbol{\theta}) = \frac{c}{H_0(1+z)} \int_0^z \frac{d\tilde{z}}{E(\tilde{z}, \boldsymbol{\theta})}. \quad (29)$$

Even in a standard scenario, the quantity $F(z)$ is independent of the parameter H_0 and can be written

$$F(z, \boldsymbol{\theta}) = \left(\int_0^z \frac{d\tilde{z}}{E(\tilde{z}, \boldsymbol{\theta})} \right) \cdot E(\tilde{z}, \boldsymbol{\theta}), \quad (30)$$

which in our notation translates into

$$F(x, \boldsymbol{\theta}) = \left(\int_1^x \frac{dx'}{a(x', \boldsymbol{\theta})} \right) \cdot \left(\frac{H(x', \boldsymbol{\theta})}{H(1, \boldsymbol{\theta})} \right), \quad (31)$$

which is independent of the parameter t_0 .

Finally, the total χ^2 to be minimized will be $\chi^2 = \chi_H^2 + \chi_{H_0}^2 + \chi_{SN}^2 + \chi_{BAO}^2$. We minimize the total χ^2 using the Markov Chain Monte Carlo (MCMC) method and we check its convergence with the method developed in [29]. In order to compare the models in the best statistical way possible, we have calculated the Bayesian evidence for each of them. The Bayesian evidence is defined as the probability of the data D given the model M with a set of parameters $\boldsymbol{\theta}$, $\mathcal{E}(M) = \int d\boldsymbol{\theta} L(D|\boldsymbol{\theta}, M) \pi(\boldsymbol{\theta}|M)$: $\pi(\boldsymbol{\theta}|M)$ is the prior on the set of parameters, normalized to unity, and $L(D|\boldsymbol{\theta}, M)$ is the likelihood function.

We have been very careful in imposing priors; our parameters are, basically, t_0 , x_s and n . Actually, we have used the parameter α defined as

$$x_s = 1 - \log_{10} \alpha \quad (32)$$

| <i>id.</i> | Ω_m | | | H_0 | t_0 | $w_{\text{eff},0}$ | \mathcal{B}_{ij} | $\log \mathcal{B}_{ij}$ |
|---------------------|----------------------------------------|-----------------------------------------|-----------------------------------------|--------------------------------------|-----------------------------------------|-----------------------------------------|--------------------|-------------------------|
| | | | | km s ⁻¹ Mpc ⁻¹ | Gyr | | | |
| ΛCDM | 0.30 ^{+0.03} _{-0.03} | | | 69.6 ^{+0.7} _{-0.7} | 13.57 ^{+0.33} _{-0.31} | -0.70 | 1 | 0 |
| <i>id.</i> | Ω_m | w_0 | w_a | H_0 | t_0 | $w_{\text{eff},0}$ | \mathcal{B}_{ij} | $\log \mathcal{B}_{ij}$ |
| | | | | km s ⁻¹ Mpc ⁻¹ | Gyr | | | |
| <i>CPL</i> | 0.36 ^{+0.05} _{-0.08} | -0.93 ^{+0.25} _{-0.25} | -1.71 ^{+2.18} _{-3.12} | 69.5 ^{+0.7} _{-0.7} | 13.29 ^{+0.39} _{-0.32} | -0.60 | 1.9 | 0.63 |
| <i>id.</i> | n | α_s | t_s | $1/t_0$ | t_0 | $w_{\text{eff},0}$ | \mathcal{B}_{ij} | $\log \mathcal{B}_{ij}$ |
| | | | t_0 | km s ⁻¹ Mpc ⁻¹ | Gyr | | | |
| <i>A</i> | 0.28 ^{+0.07} _{-0.06} | 0.27 ^{+0.17} _{-0.16} | 2.30 ^{+0.61} _{-0.58} | 69.9 ^{+1.6} _{-1.7} | 13.99 ^{+0.36} _{-0.32} | -0.72 ^{+0.12} _{-0.12} | 1.5 | 0.42 |
| <i>B</i> | 0.34 ^{+0.07} _{-0.07} | 0.42 ^{+0.21} _{-0.23} | 1.86 ^{+0.50} _{-0.54} | 69.4 ^{+1.7} _{-1.7} | 14.10 ^{+0.35} _{-0.33} | -0.69 ^{+0.11} _{-0.11} | 1.6 | 0.48 |
| <i>C</i> | 0.99 ^{+0.57} _{-0.39} | < 0.28 | > 2.28 | 71.8 ^{+1.4} _{-1.4} | 13.62 ^{+0.27} _{-0.27} | -0.91 ^{+0.22} _{-0.22} | 2.5 | 0.90 |
| <i>D</i> | 0.72 ^{+0.11} _{-0.08} | < 0.27 | > 2.32 | 66.6 ^{+1.9} _{-2.0} | 14.70 ^{+0.45} _{-0.41} | -0.49 ^{+0.05} _{-0.05} | 13.5 | 2.60 |
| <i>E</i> | 0.96 ^{+0.19} _{-0.14} | < 0.10 | > 3.33 | 65.2 ^{+2.1} _{-2.2} | 15.01 ^{+0.53} _{-0.47} | -0.44 ^{+0.06} _{-0.06} | 43.6 | 3.78 |

Table II. In this table we present the obtained results for the best fit of each parameterization. In column 1 we give the label identifying each parameterization in Table I. In columns 2-5 we give the 1σ confidence levels for our primary model parameters. In column 6 we show the age of the Universe. We also show the effective equation of state parameter (as defined in (17)) for each parameterization evaluated at the present. Finally, in columns 8 and 9 we give the Bayesian evidence and ratio with respect to ΛCDM for Jeffreys' interpretation.

in order to compactify the range $x_s \in (1, \infty)$ into $\alpha \in (0, 1)$. We have imposed a flat prior on α on this range, while for n (and t_0) we assume a flat prior for only positive values, $n > 0$, given that this is the condition to ensure present accelerated expansion for all the models. The only exception is for the singularity D, where acceleration is guaranteed for $n > \bar{n}(\alpha) > 0$, with $\bar{n}(\alpha)$ numerically found imposing the condition $q(t) = 0$, with $q(t)$ being the deceleration parameter. Thus, the parameters span sufficiently wide and general ranges in order to have the same weight for each model when calculating the Bayesian evidence. The evidence is estimated using the algorithm in [30]; in order to reduce the statistical noise we run the algorithm many times obtaining a distribution of ~ 100 values from which we extract the best value of the evidence as the mean of such distribution.

In order to compare the goodness of the different parameterizations, we further calculate the Bayes Factor, defined as the ratio of evidences of two models, M_i and M_j , $\mathcal{B}_{ij} = \mathcal{E}_i/\mathcal{E}_j$. If $\mathcal{B}_{ij} > 1$, model M_i is preferred over M_j , given the data. We will use the ΛCDM model as the reference model i (we have performed a further analysis with this model using the same data sets we have described above). The Bayesian evidence may be interpreted using Jeffreys' Scale [31], which tries to quantify the preference of a model against another based on the value of the evidence. In particular, if the $\ln \mathcal{B}_{ij} < 1$, the evidence in favor of the highest-evidence model is not significant; if $1 < \ln \mathcal{B}_{ij} < 2.5$, the evidence is substantial; if $2.5 < \ln \mathcal{B}_{ij} < 5$, the evidence is strong; and if $\ln \mathcal{B}_{ij} > 5$,

the evidence is decisive. In [32], it is shown that the Jeffreys' scale is not a fully-reliable tool for model comparison, but at the same time the statistical validity of the Bayes factor as an efficient model-comparison tool is not questioned: a Bayes factor $\mathcal{B}_{ij} > 1$ unequivocally states that the model i is more likely than model j . We present results in both contexts for reader's interpretation.

V. RESULTS

After the datasets introduced in the previous section and the discussed considerations, we have proceeded to run the MCMC chains in order to obtain the confidence regions of each parameterization and, therefore, achieving the main goal of this work, namely, obtaining a lower bound for the time of a future singularity. The results corresponding to our different cases are shown in Fig. 1, where we display the marginalized contours of the parameters for each model, and in Table II. In order to have a further criterium to judge the statistical validity of our models, we have also analyzed, using the same data sets we have described in the previous section, the ΛCDM model and the Chevallier-Polarski-Linder (CPL) parametrization [33], which is widely used as the most basic generalization of a constant dark energy to a dynamical fluid.

When considering the combination of all the datasets, we obtain that the lowest value for the singularity time is achieved for model B and turns out to be $t_{s,\text{min}} \simeq 1.2$

(at the 2σ level), which corresponds to 2.8 Gyrs from today. Remarkably, this time is shorter than the expected time for the Sun to burn all its fuel (estimated to be 5-7 Gyrs). Although model B gives the lowest allowed value for the time of the singularity, it is interesting to note that models A, B, C and D consistently give a lower bound for t_s in the range $1.2t_0 - 1.5t_0$ (still smaller than the remaining life of the Sun), while model E only allows for $t_s \gtrsim 2.5t_0$.

An interesting feature of models A and B is that having the singularity at infinity is excluded at the 1σ level. We should remember that t_s corresponds to having a de Sitter universe in the asymptotic future, so for those two models, such a scenario is disfavoured. This highlights our discussion on the fact that having an asymptotically de Sitter universe in our parameterizations does not necessarily implies being close to a Λ CDM model. Remarkably, these two models present a Bayesian evidence which make them equivalent to Λ CDM from a statistical point of view, i.e., they provide fits as good as those of Λ CDM, and they are also equivalent (or even slightly better) than the more classical and most used CPL parametrization. Notice moreover that the effective equation of state parameter today is close to the one of Λ CDM.

For model C, the possibility of having the singularity at infinity is within the 1σ region. The Bayesian evidence in this case is slightly higher than for A and B, but still not strongly disfavoured with respect to Λ CDM. Interestingly the effective equation of state parameter today for this case is substantially higher than for Λ CDM.

Finally, models D and E are strongly disfavoured with respect to the baseline Λ CDM. Again, these models allow to have $t_s = \infty$ at the 1σ level. In these cases, we find that $w_{\text{eff},0}$ is lower than in the Λ CDM case.

VI. CONCLUSION

In this work we have reconsidered the subject of future cosmological singularities occurring at a finite time. The aim of the work has been to establish a general lower bound for the time of a potential future singularity by using SN Ia, BAO and $H(z)$ data. We have briefly reviewed the cosmological singularities emphasizing the fact that a divergence in a given cosmological parameter does not necessarily implies a singular spacetime. We have then discussed under which conditions a given *cosmological* singularity actually corresponds to a *singular*

spacetime so that we can discern the severity of the different cosmological singularities. Our discussion focused on the geodesic completeness of the spacetime as well as the presence of divergent tidal forces when approaching the singularity.

After this brief theoretical review, we have constructed a set of parameterizations comprising different types of singularities. These parameterizations have been designed so that we recover an early time matter dominated phase that transits to a phase with a future singularity where a given time-derivative of the scale factor diverges, but not the lower ones. We have then run a series of MCMC chains to confront our parameterizations to SN Ia, BAO and $H(z)$ data. The obtained results are then summarized in Table. II. Our main conclusion is that quite generally a potential future singularity cannot be closer to the present time than $\sim 0.2t_0$, that roughly corresponds to 2.8 Gyr. We found that the proximity of the singularity to the present time has a mild dependence on the type of singularity for our parameterizations, but we can conclude that in all cases there is a consistent lower bound around $1.2 - 1.5t_0$.

Another interesting conclusion that we have found is that, following results from the Bayesian evidence, our parameterizations A and B are provide fits statistically equivalent in goodness to Λ CDM. This was not obvious a priori since none of our parameterizations contain Λ CDM in its parameter space. Hence, as shown in previous references [17], a singular scenario can not be discarded and the time remaining for the occurrence of a future singularity may be shorter than expected.

Acknowledgments: We thank Antonio L. Maroto and Diego Rubiera-Garcia for fruitful discussions and comments. J.B.J. acknowledges the financial support of A*MIDEX project (n ANR-11-IDEX-0001-02) funded by the Investissements dAvenir French Government program, managed by the French National Research Agency (ANR), MINECO (Spain) projects FIS2011-23000, FIS2014-52837-P and Consolider-Ingenio MULTIDARK CSD2009-00064. V.S. is financed by the Polish National Science Center Grant DEC-2012/06/A/ST2/00395. D.S.G. acknowledges support from a postdoctoral fellowship Ref. SFRH/BPD/95939/2013 by Fundação para a Ciência e a Tecnologia (FCT, Portugal) and the support through the research grant UID/FIS/04434/2013 (FCT, Portugal).

[1] E. J. Copeland, M. Sami and S. Tsujikawa, *Int. J. Mod. Phys. D* **15**, 1753 (2006) doi:10.1142/S021827180600942X [hep-th/0603057]; K. Bamba, S. Capozziello, S. Nojiri and S. D. Odintsov, *Astrophys. Space Sci.* **342**, 155 (2012) [arXiv:1205.3421 [gr-qc]]; S. Nojiri and S. D. Odintsov, *Phys. Rept.* **505**, 59 (2011) [arXiv:1011.0544 [gr-qc]]; *eConf C* **0602061**

(2006) 06 [Int. J. Geom. Meth. Mod. Phys. **4** (2007) 115] [hep-th/0601213]; L. Amendola, *Dark Energy: Theory and Observations*, Cambridge Press 2015; *Phys. Rept.* **509**, 167 (2011) [arXiv:1108.6266 [gr-qc]]; P. J. E. Peebles and B. Ratra, *Rev. Mod. Phys.* **75**, 559 (2003) doi:10.1103/RevModPhys.75.559 [astro-ph/0207347]. F. S. N. Lobo, *Dark Energy-Current Advances and Ideas*

- [arXiv:0807.1640 [gr-qc]];
- [2] R.R. Caldwell, R. Dave, and P.J. Steinhardt, *Phys. Rev. Lett.* **80**, 1582 (1998); E. Elizalde, S. Nojiri and S. D. Odintsov, *Phys. Rev. D* **70**, 043539 (2004) [hep-th/0405034]. S. Capozziello, S. Nojiri, and S. D. Odintsov, *Phys. Lett. B* **632**, 597 (2006) [arXiv:hep-th/0507182]; S. Nojiri and S. D. Odintsov, *Gen. Rel. Grav.* **38**, 1285 (2006) [arXiv:hep-th/0506212]; S. Nojiri, S. D. Odintsov and H. Stefancic, *Phys. Rev. D* **74**, 086009 (2006) [hep-th/0608168]; E. Elizalde, S. Nojiri, S. D. Odintsov, D. Saez-Gomez and V. Faraoni, *Phys. Rev. D* **77**, 106005 (2008), [arXiv:0803.1311 [hep-th]]; S. Carloni, S. Capozziello, J. A. Leach and P. K. S. Dunsby, *Class. Quant. Grav.* **25**, 035008 (2008) [gr-qc/0701009]. E. N. Saridakis and S. V. Sushkov, *Phys. Rev. D* **81**, 083510 (2010) [arXiv:1002.3478 [gr-qc]]. T. Harko, F. S. N. Lobo and M. K. Mak, *Eur. Phys. J. C* **74**, 2784 (2014) [arXiv:1310.7167 [gr-qc]];
- [3] B. Elder, A. Joyce and J. Khoury, *Phys. Rev. D* **89** (2014) 4, 044027 doi:10.1103/PhysRevD.89.044027 [arXiv:1311.5889 [hep-th]]. V. A. Rubakov, *Phys. Usp.* **57** (2014) 128 doi:10.3367/UFNe.0184.201402b.0137 [arXiv:1401.4024 [hep-th]].
- [4] S. Nojiri and S. D. Odintsov, *Phys. Rept.* **505**, 59 (2011) [arXiv:1011.0544 [gr-qc]]; eConf C **0602061** (2006) 06 [Int. J. Geom. Meth. Mod. Phys. **4** (2007) 115] [hep-th/0601213]; S. Capozziello and V. Faraoni, *Beyond Einstein Gravity*, Springer, Dordrecht, (2010) ;
- [5] P. H. Frampton, K. J. Ludwick and R. J. Scherrer, *Phys. Rev. D* **84**, 063003 (2011) doi:10.1103/PhysRevD.84.063003 [arXiv:1106.4996 [astro-ph.CO]]; S. Nojiri, S. D. Odintsov and D. Saez-Gomez, *AIP Conf. Proc.* **1458**, 207 (2011) doi:10.1063/1.4734414 [arXiv:1108.0767 [hep-th]].
- [6] P. H. Frampton, K. J. Ludwick and R. J. Scherrer, *Phys. Rev. D* **85**, 083001 (2012) doi:10.1103/PhysRevD.85.083001 [arXiv:1112.2964 [astro-ph.CO]].
- [7] M. Bouhmadi-Lopez, A. Errahmani, P. Martin-Moruno, T. Ouali and Y. Tavakoli, *Int. J. Mod. Phys. D* **24**, no. 10, 1550078 (2015) doi:10.1142/S0218271815500789 [arXiv:1407.2446 [gr-qc]].
- [8] S. Nojiri, S. D. Odintsov and S. Tsujikawa, *Phys. Rev. D* **71**, 063004 (2005) [hep-th/0501025].
- [9] L. Fernandez-Jambrina, *Phys. Rev. D* **90**, 064014 (2014) [arXiv:1408.6997 [gr-qc]].
- [10] S. Hawking and G. Ellis, *The Large Scale Structure of Space-Time*, Cambridge University Press 1973.
- [11] A. Tilquin and T. Schucker, arXiv:1508.00809 [astro-ph.CO].
- [12] F. J. Tipler, *Phys. Lett. A* **64** (1977) 8. doi:10.1016/0375-9601(77)90508-4
- [13] A. Krolak, *Class. and Quantum Grav.* **3** 267 (1986).
- [14] R. R. Caldwell, M. Kamionkowski and N. N. Weinberg, *Phys. Rev. Lett.* **91**, 071301 (2003) [astro-ph/0302506].
- [15] M. P. Dabrowski, K. Marosek, *JCAP* **02** (2013) 012.
- [16] M. Bouhmadi-Lopez and J. A. Jimenez Madrid, *JCAP* **0505**, 005 (2005) doi:10.1088/1475-7516/2005/05/005 [astro-ph/0404540]; P. X. Wu and H. W. Yu, *Nucl. Phys. B* **727**, 355 (2005) doi:10.1016/j.nuclphysb.2005.07.022 [astro-ph/0407424]; A. V. Astashenok, S. Nojiri, S. D. Odintsov and A. V. Yurov, *Phys. Lett. B* **709**, 396 (2012) doi:10.1016/j.physletb.2012.02.039 [arXiv:1201.4056 [gr-qc]]; B. McInnes, *JHEP* **0208**, 029 (2002) doi:10.1088/1126-6708/2002/08/029 [hep-th/0112066].
- [17] R. Lazkoz, R. Maartens and E. Majerotto, *Phys. Rev. D* **74**, 083510 (2006) [astro-ph/0605701]. S. Nesseris and L. Perivolaropoulos, *JCAP* **0701**, 018 (2007) [astro-ph/0610092]. C. Kaeonikhom, B. Gumjudpai and E. N. Saridakis, *Phys. Lett. B* **695**, 45 (2011) [arXiv:1008.2182 [astro-ph.CO]]. B. Novosyadlyj, O. Sergijenko, R. Durrer and V. Pelykh, *Phys. Rev. D* **86**, 083008 (2012) [arXiv:1206.5194 [astro-ph.CO]]; *JCAP* **06** (2013) [arXiv:1212.5824 [astro-ph.CO]]; I. Leanizbarrutia and D. Sáez-Gómez, *Phys. Rev. D* **90**, no. 6, 063508 (2014) [arXiv:1404.3665 [astro-ph.CO]].
- [18] L. Fernandez-Jambrina and R. Lazkoz, *Phys. Rev. D* **74**, 064030 (2006) doi:10.1103/PhysRevD.74.064030 [gr-qc/0607073].
- [19] J. D. Barrow, *Class. Quant. Grav.* **21**, L79 (2004), gr-qc/0403084. J. D. Barrow, *Class. Quant. Grav.* **21**, 5619 (2004), gr-qc/0409062; J. D. Barrow, G. J. Galloway and F. J. Tipler *Mon. Not. Roy. Astr. Soc.* **223**, 835-844 (1986)
- [20] M. Bouhmadi-Lopez, P. F. Gonzalez-Diaz and P. Martin-Moruno, *Phys. Lett. B* **659**, 1 (2008) [gr-qc/0612135].
- [21] M. P. Dabrowski, K. Marosek and A. Balcerzak, *Mem. Soc. Ast. It.* **85**, no. 1, 44 (2014) [arXiv:1308.5462 [astro-ph.CO]].
- [22] M. P. Dabrowski and T. Denkiwicz, *Phys. Rev. D* **79**, 063521 (2009) [arXiv:0902.3107 [gr-qc]]. M. P. Dabrowski and T. Denkiwicz, *AIP Conf. Proc.* **1241**, 561 (2010) [arXiv:0910.0023 [gr-qc]]; L. Fernandez-Jambrina, *Phys. Lett. B* **656**, 9 (2007) [arXiv:0704.3936 [gr-qc]].
- [23] L. Fernandez-Jambrina and R. Lazkoz, *Phys. Rev. D* **70** (2004) 121503 doi:10.1103/PhysRevD.70.121503 [gr-qc/0410124].
- [24] M. P. Dabrowski, *Phys. Rev. D* **71** (2005) 103505; M. P. Dabrowski, T. Denkiwicz, M. A. Hendry, *Phys. Rev. D* **75** (2007) 123524; H. Godsi, M. A. Hendry, M. P. Dabrowski, T. Denkiwicz, *MNRAS* **414** (2011) 1517; T. Denkiwicz, M. P. Dabrowski, H. Godsi, M. A. Hendry, *Phys. Rev. D* **85** (2012) 083527; M. P. Dabrowski, K. Marosek, *JCAP* **02** (2013) 012;
- [25] M. Moresco, *MNRAS* **450** (2015) 1.
- [26] C. L. Bennett, D. Larson, J. L. Weiland, G. Hinshaw, *ApJ* **794** (2014) 135.
- [27] N. Suzuki, et al., *ApJ* **746** (2012) 85.
- [28] C. Blake, et al., *MNRAS* **425** (2012) 405.
- [29] J. Dunkley, M. Bucher, P. G. Ferreira, K. Moodley, C. Skordis, *MNRAS* **356** (2005) 925.
- [30] P. Mukherjee, D. Parkinson, A. R. Liddle, *Astrophys. J.* **638** (2006) 51.
- [31] H. Jeffreys, "The theory of probability", Oxford U. P. (1998).
- [32] S. Nesseris, J. Garcia - Bellido, *JCAP* **08** (2013) 036.
- [33] M. Chevallier, D. Polarski, *Int. J. Mod. Phys. D.* **10**, 213 (2001); E. V. Linder, *Phys. Rev. Lett.* **90**, 091301 (2003).

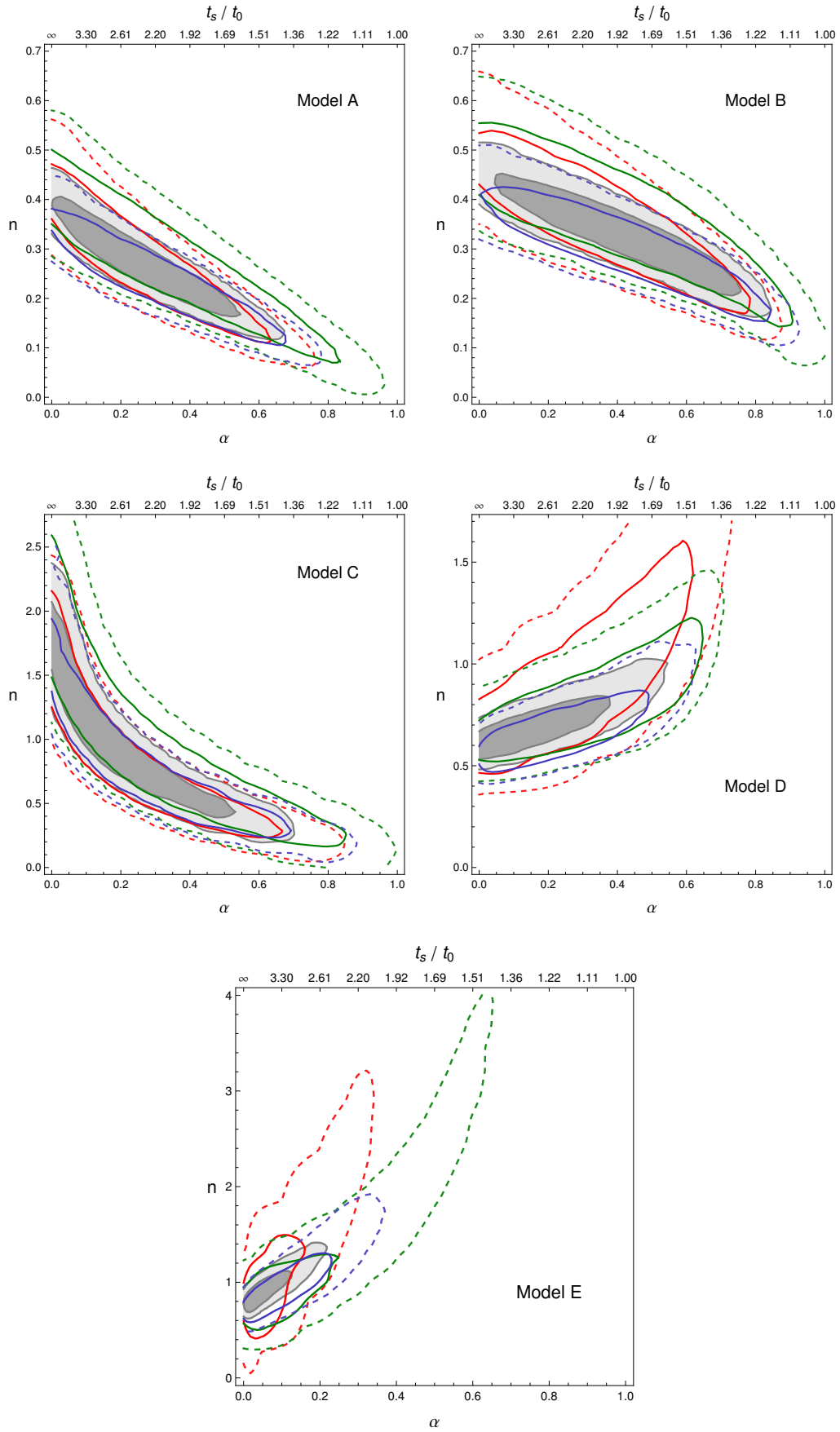


Figure 1. Results: 68% and 95% confidences level for n and α . Red: supernovae; green: BAO; blue: Hubble data; grey: total combined data sets. From left to right and from top to bottom: singularity A; singularity B; singularity C; singularity D; singularity E.

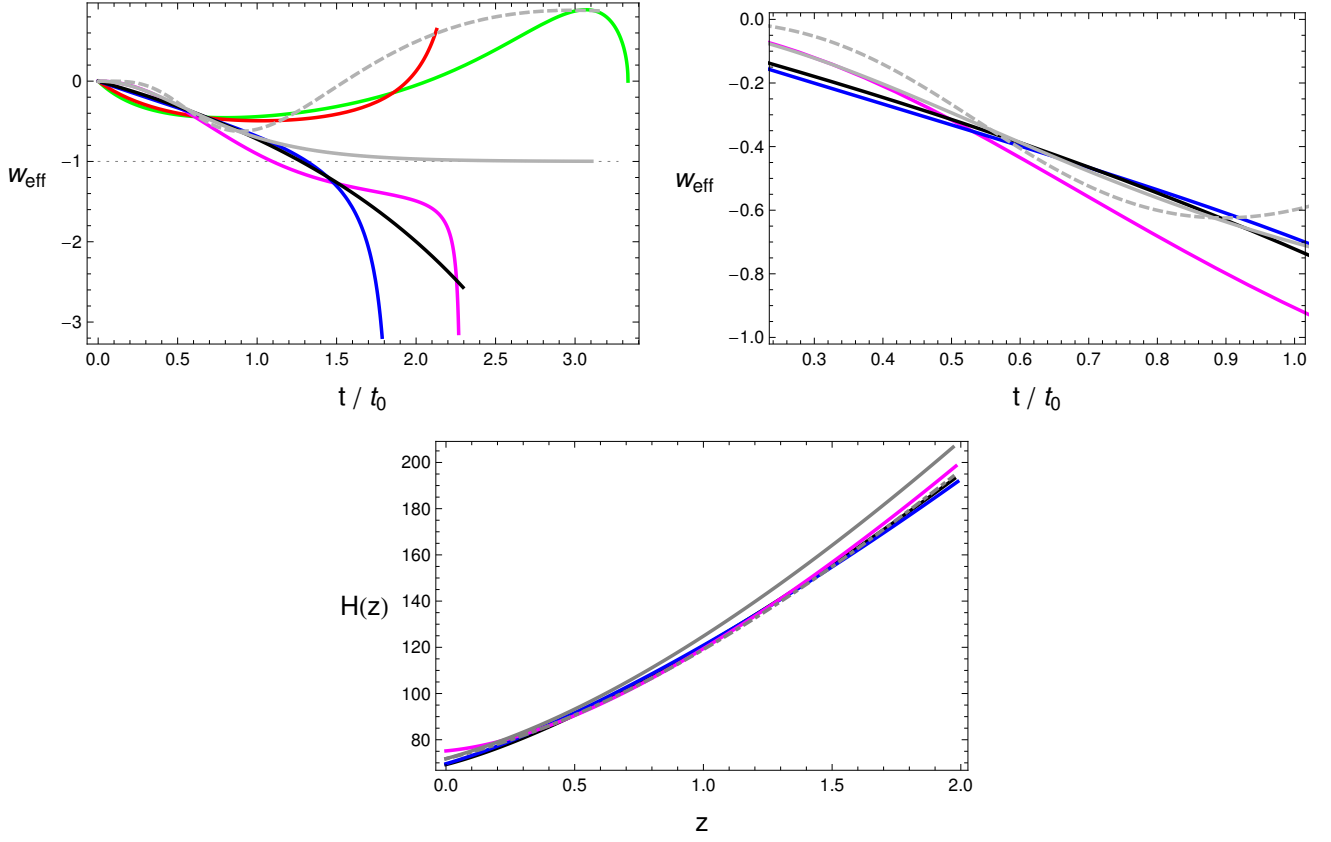


Figure 2. (*Top Panel:*) Effective EoS for the combined effect of matter and “singularity-fluid”. Λ CDM from Table: solid light grey - CPL from Table: dashed light grey - Singularity A: black - Singularity B: blue - Singularity C: magenta - Singularity D: red - Singularity E: green. (Left: all models for all times - Right: zoom of the best models in the approximate time range covered by data). (*Bottom Panel:*) Rate expansion in terms of redshift, $H(z)$, in the approximate range covered by data. Λ CDM from Table: solid light grey - Λ CDM with H_0 from Table and $\Omega_{m,0} \sim 0.25$ visually-varied in order to fit our models: dotted light grey - Singularity A: black - Singularity B: blue - Singularity C: magenta.